Global loss of imprinting leads to widespread tumorigenesis in adult mice

Teresa M. Holm,[1,2] Laurie Jackson-Grusby,[1,3] Tobias Brambrink,[1] Yasuhiro Yamada,[1,4] William M. Rideout III,[1,5] and Rudolf Jaenisch[1,2,*]

[1]Whitehead Institute for Biomedical Research, Cambridge, Massachusetts 02142
[2]Massachusetts Institute of Technology, Cambridge, Massachusetts 02142
[3]Present address: Pathology Department, Children's Hospital Boston and Harvard Medical School, 320 Longwood Avenue, Boston, Massachusetts 02115
[4]Present address: Department of Tumor Pathology, Gifu University, Gifu 501-1194, Japan
[5]Present address: AVEO Pharmaceuticals Inc., Cambridge, Massachusetts 02139
*Correspondence: jaenisch@wi.mit.edu

Summary

Loss of imprinting (LOI), commonly observed in human tumors, refers to loss of monoallelic gene regulation normally conferred by parent-of-origin-specific DNA methylation. To test the function of LOI in tumorigenesis, we developed a model by using transient demethylation to generate imprint-free mouse embryonic stem cells (IF-ES cells). Embryonic fibroblasts derived from IF-ES cells (IF-MEFs) display TGFβ resistance and reduced p19 and p53 expression and form tumors in SCID mice. IF-MEFs exhibit spontaneous immortalization and cooperate with H-Ras in cellular transformation. Chimeric animals derived from IF-ES cells develop multiple tumors arising from the injected IF-ES cells within 12 months. These data demonstrate that LOI alone can predispose cells to tumorigenesis and identify a pathway through which immortality conferred by LOI lowers the threshold for transformation.

Introduction

Cancer has traditionally been thought to be caused by a series of genetic mutations in cancer susceptibility genes, which include oncogenes, tumor suppressor genes, and genes causing genetic instability. Until recently, this rationale has remained relatively unchallenged. However, it is now clear that epigenetic changes (changes to the DNA maintained by cell division other than alterations to the nucleotide sequence) play a critical role during tumorigenesis (Feinberg and Tycko, 2004). The genome of cancer cells is characterized by localized hypermethylation in CpG islands, resulting in the silencing of tumor suppressor gene expression (Baylin and Bestor, 2002). In addition, global genomic and CpG island hypomethylation are associated with both benign and malignant tumors (Feinberg and Vogelstein, 1983a; Gama-Sosa et al., 1983). Mechanistically, these epigenetic changes are known to cause both oncogene activation and chromosomal instability resulting in loss of heterozygosity (Feinberg and Vogelstein, 1983b; Chen et al., 1998; Gaudet et al., 2003).

Imprinted genes display a characteristic parent-of-origin-specific DNA methylation pattern that results in only a single allele being expressed (either the paternal or maternal allele). DNA methylation that maintains the monoallelic expression of imprinted genes is established during gametogenesis and is important for fetal growth regulation and perinatal development (Bartolomei, 2003; Reik and Walter, 2001). Although imprinting persists in the adult, the requirements for proper imprinting in the context of normal tissue homeostasis is not well understood.

Loss of imprinting (LOI), either biallelic expression or complete silencing of imprinted genes, has been implicated in the progression of several tumors (Ogawa et al., 1993; Rainier et al., 1993). For instance, aberrant biallelic expression of the *Insulin-like growth factor-2* (*IGF2*) gene, a significant risk factor for human colorectal carcinogenesis, is thought to promote tumorigenesis by inhibiting apoptosis (Cui et al., 2003). In addition *PEG3*, *P57*, and *IGF2R* all display LOI that leads to their silencing in oligodendrogliomas, breast cancer, and hepatocellular carcinomas, respectively (De Souza et al., 1997; Kobatake et al., 2004; Trouillard et al., 2004). Although there is evidence that LOI at the *IGF2* locus promotes tumorigenesis in Beckwith-Wiedemann syndrome (DeBaun et al., 2002), for the majority of human tumors it has not been clear if LOI plays a

SIGNIFICANCE

Loss of the DNA methylation associated with specific imprinted genes is a common feature of human cancers. However, it has not been clear if a global loss of imprinting (LOI) in untransformed cells would predispose them to tumorigenesis. We now report evidence to support a model in which LOI at key loci encoding tumor suppressors and oncogenes provides the first step toward tumor formation by conferring cellular immortality. Subsequent genetic alterations, such as constitutive activation of a mitogenic signal, would then provide the next step necessary for a fully transformed phenotype.

causal role in cancer or is merely a consequence of altered epigenetic regulation in already transformed cells. Furthermore, in all studies to date, the effects of LOI on cancer progression have either been analyzed at single imprinted loci using association studies in humans and mutational analysis in mice or have examined the consequences of a global imbalance of maternal and paternal imprints in animals derived from parthenogenetic or androgenetic cells, respectively (Hernandez et al., 2003). Thus, the effect of genome-wide LOI on tumor formation has not been addressed.

Here, we use conditional alleles of *Dnmt1*, which encodes a DNA methyl transferase, to transiently remove all DNA methylation marks from the genome of embryonic stem (ES) cells. Reactivation of *Dnmt1* expression resulted in a restoration of global DNA methylation but failed to remethylate imprinted genes. From these imprint-free (IF) ES cells, we derived murine embryonic fibroblasts (MEFs) and examined their growth characteristics. The IF-MEFs displayed a number of characteristics of transformed cells, including increased growth rate, immortality, and resistance to growth inhibition by TGFβ. When injected into severe combined immunodeficient (SCID) mice, the IF-MEFs formed tumors with long latency. Overexpression of oncogenic V12H-Ras in the IF-MEFs significantly shortened tumor latency. Chimeric animals that were generated with the IF-ES cells developed widespread tumors by 12 months of age, with the cancers being derived from the IF-ES cells. Our findings suggest a causal link between LOI and cancer and demonstrate that imprinting plays a critical tumor suppressor role in the adult.

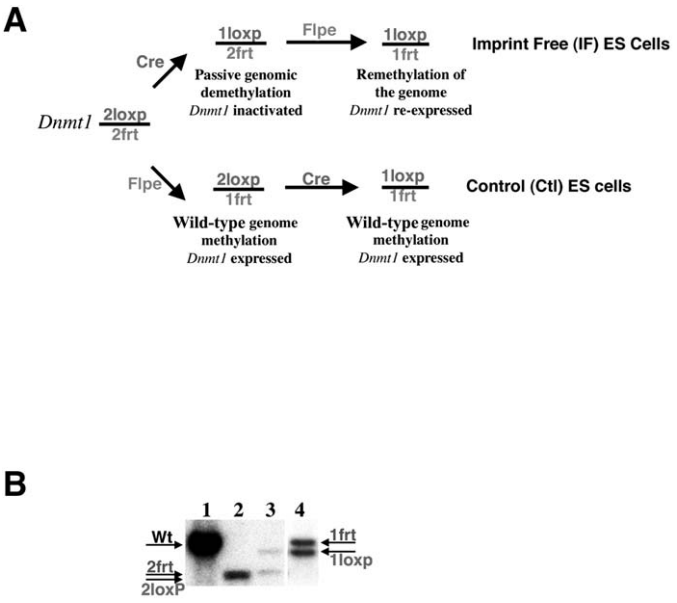

Figure 1. Generation of IF- and CTL-ES cells

A: Schematic representation of the steps used to create the IF-ES cells (for specific alleles and the status of global genomic methylation at each stage, see Figure S1). CTL-ES cells were generated by reverse exposure to the recombinases.

B: Genomic Southern blot analysis confirming the recombined DNMT1 alleles. Lane 1, wild-type Dnmt1; lane 2, 2loxp/2frt Dnmt1; lane 3, 1loxp/2frt Dnmt1; lane 4, 1loxp/1frt Dnmt1.

Results

Generation of IF- and CTL-ES cells

To investigate the role of LOI in the progression of cancer, we took advantage of previous observations in which mouse ES cells deficient in *Dnmt1* (encoding an enzyme that maintains global DNA methylation) were found to lack global DNA methylation, including the methylation associated with imprinting (Li et al., 1993). Although loss of *Dnmt1* through a conditional knockout allele has no effect on ES cell viability, it is essential in differentiated cells (Jackson-Grusby et al., 2001). Lethality and global DNA methylation have been rescued following reexpression of a *Dnmt1* cDNA in the *Dnmt1* mutant ES cells (Tucker et al., 1996b). However, because of the low *Dnmt1* level in the "rescued" cells, the genome was incompletely remethylated, resulting in abnormalities such as genomic instability (Chen et al., 1998; Gaudet et al., 2003). To circumvent these shortcomings, and to generate ES cells expressing normal and properly regulated levels of *Dnmt1*, we devised an alternative strategy in which *Dnmt1* was first conditionally inactivated and then reactivated by sequential exposure of the cells to the Cre and flp recombinases. To do this, we constructed an inactive *Dnmt1* allele (2frt) by inserting a stop cassette flanked by two Frt sites between the fourth and fifth exons of the *Dnmt1* gene. This mutant allele is revertible and becomes reactivated following Flp-mediated recombination (Figure 1A; Figure S1 in the Supplemental Data available with this article online). Mice carrying the 2frt allele were generated by injection of targeted ES cells into mouse blastocysts, and the subsequent animals were bred to the *Dnmt1* 2lox (Jackson-Grusby et al., 2001) and a ROSA26 Flp reporter allele (Possemato et al., 2002). ES cell lines containing the *Dnmt1* conditional 2lox and *Dnmt1* 2frt alleles and the Flp β-geo reporter allele were derived from these animals (Figure 1A). When the 2lox/2frt ES cells were transfected with a Cre plasmid, deletion of exons 4 and 5 created the null *Dnmt1* 1lox allele, resulting in *Dnmt1* deficiency (Figure 1B). Consistent with this, the 1lox/2frt cells displayed global genome demethylation as demonstrated by Southern blot analysis of centromeric regions, LINE, and IAP elements (Figure S1). The demethylated cells were then transfected with a Flpe plasmid, causing the stop cassette to be excised (2frt → 1frt), the *Dnmt1* allele to be reactivated, and genome methylation to be restored (Figure 1A; Figure S1; these cells are herein referred to as "IF-ES cells") (Buchholz et al., 1998). To serve as a control, we transfected 2lox/2frt ES cells with Flpe first and Cre second, a manipulation that maintains *Dnmt1* activity at each step and has no effect on genomic methylation level and imprinting (referred to as "CTL-ES cells") (Figure 1A).

Expression and methylation of IF- and CTL-MEFs

To confirm that our strategy had successfully erased imprinting, we examined the methylation status of selected imprinted genes in IF-ES cells and MEFs. To generate the MEFs, wild-type blastocysts were injected with either IF- or CTL-ES cells, and fibroblasts were isolated from E13.5 chimeras using G418 resistance to select for ES cell-derived MEFs. As assessed by Southern blot analysis, the restoration of normal global methylation was maintained in the MEFs (Figures S1Ca–S1Cc). LOI at the *Igf2r*, *Snrpn*, *Peg3*, and *Igf2* loci was assessed by methylation-sensitive Southern blotting and COBRA analysis (Xiong

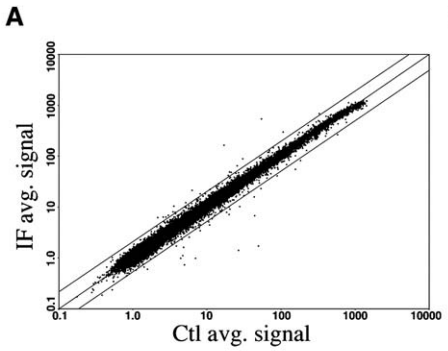

B

Fold Regulation-UP		Fold Regulation-Down	
Impact	↑1.7	Igf2r	↓2.5
Plagl1	↑2.2	Grb10/Meg1	↓10
Sgce	↑1.6	Ctgf	↓2.7
Peg12/Frat	↑1.4	p57kip2/cdkn1c	↓3.5
Ndn	↑1.6	Zim1	↓not expressed
Peg3	↑1.8	Thrombospondin	↓2.1
Igf2	var	H19	var

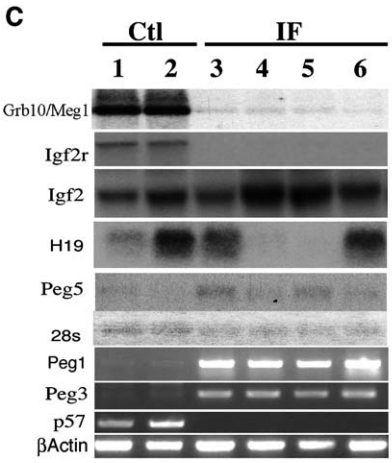

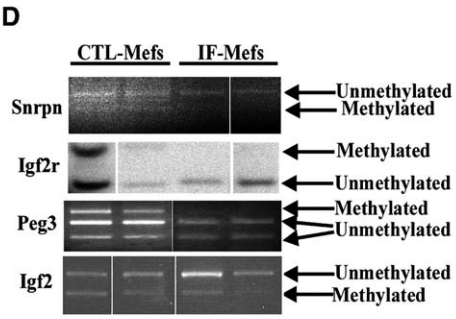

Figure 2. Characterization of IF- and CTL-MEFs

A: Characterization of IF- and CTL-MEFs by microarray analysis.

B: Selected imprinted genes that are up- or downregulated in IF-MEFs by microarray analysis. p values: impact, 0.118; Plagl1, 0.040; Sgce, 0.118; Ndn, 0.069; Peg3, 0.383; Igf2r, 0.145; Grb10/Meg1, 0.128; Ctgf, 0.002; Zim1, 0.228; Thrombospondin, 0.0005.

C: Confirmation of the expression of selected imprinted genes by Northern blot and RT-PCR analysis. Lanes 1 and 2, CTL-MEFs; lanes 3, 4, 5, and 6, IF-MEFs.

D: Methylation status of imprinted genes in CTL- and IF-MEFs. Carried out by methylation-sensitive Southern blot analysis for Igf2r and COBRA analysis for Igf2, Snrpn, and Peg3.

and Laird, 1997). While normal imprinted methylation of *Igf2r*, *Snrpn*, and *Peg3* was found in the CTL-ES cells and CTL-MEFs, these genes lacked methylation in IF-ES cells and IF-MEFs, consistent with LOI. In contrast, COBRA analysis revealed that the differentially methylated region (DMR) of the *Igf2-H19* locus, a regulatory element that controls expression of *H19* and *Igf2*, was variably methylated in IF-ES cells and IF-MEFs (Figure 2D). Although this result was contrary to expectation in our model, it was not surprising, since the *Igf2-H19* DMR is highly susceptible to de novo methylation when the methylation status of the genome has been altered (Baqir and Smith, 2003; Biniszkiewicz et al., 2002; Chen et al., 1998; Tucker et al., 1996b), whereas the methylation status of other imprinted regions is more stable. Loss of the DNA methylation associated with imprinting is expected to either erase or result in biallelic expression of imprinted genes, depending on whether the methylation of the respective imprinting box or DMR has a positive or negative effect on transcription (Reik and Walter, 2001). To assess the effect of LOI on gene expression, we examined the gene expression profiles of IF-MEFs and CTL-MEFs using microarrays. This analysis revealed a tight clustering for most genes, indicating that there was very little difference in expression patterns between the two populations (Pearson coefficient r = 0.9919) (Figure 2A). However, the expression of a small number of genes, mostly corresponding to known imprinted genes, was altered (Figure 2B). The remaining genes were known or likely downstream targets of imprinted genes (data not shown), although we cannot rule out the possibility that some represent non-imprint-related genes independently affected by our demethylation/remethylation strategy. In agreement with our finding that the *Igf2-H19* DMR was variably methylated, we found that the level of *Igf2* was ~2-fold higher and that there was no *H19* expression in two of four IF-MEF samples as compared to CTL-MEFs, and the other two IF-MEFs were unchanged relative to the CTL-MEFs. To validate the microarray data, expression of *Meg1/Grb10*, *Igf2r*, *Igf2*, *H19*, *Peg5*, *Peg1*, *Peg3*, and *p57* was examined in the IF- and CTL-MEFs by Northern blot analysis and RT-PCR, as described in the Experimental Procedures (Figure 2C). This analysis confirmed that the IF-MEFs were negative for *Igf2r*, *Meg1/Grb10*, and *p57* and variable for *H19* but displayed increased levels of *Peg3*, *Peg5*, and variable *Igf2* compared to CTL-MEFs. Our findings suggest that the strategy of conditionally inactivating and then reactivating *Dnmt1* successfully erased the methylation associated with imprinting, but not global genome methylation, resulting in widespread alterations in the expression of imprinted genes.

Altered growth properties of IF-MEFs

Many imprinted genes, such as *Igf2* and *Grb10/Meg1*, have been implicated in embryonic growth control (Reik and Walter, 2001). We therefore examined whether IF-MEFs displayed altered growth properties compared to CTL-MEFs. To analyze the cell cycle in the MEFs, DNA content was measured by flow cytometry. The majority (~70%) of the CTL-MEFs were in the G_1 phase of the cell cycle, with approximately 13% and 17%

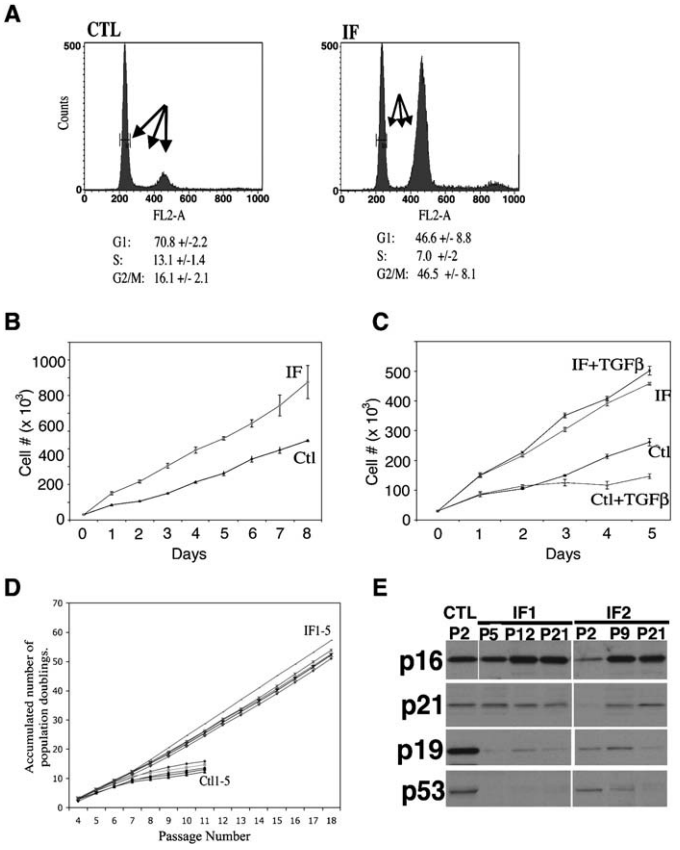

Figure 3. Growth characteristics and immortalization of IF-MEFs

A: Cell cycle analysis of IF- and CTL-MEFs by flow cytometry. A representative example of propidium iodide-stained MEFs is shown for both IF and CTL. The three arrows indicate the peaks that represent cells in G_1, S, and G_2/M phase of the cell cycle, respectively. Below each graph is the quantification of cells in each stage of the cell cycle.

B: Growth rate of IF- and CTL-MEFs. The graph shows the faster growth rate of IF-MEFs (9.3×10^4 cells/day) compared to CTL-MEFs (5.7×10^4 cells/day) over a period of 8 days. Day 1: IF-MEFs, 149.5 ± 4.5; CTL-MEFs, 84.5 ± 6.2. Day 2: IF-MEFs, 216 ± 4.1; CTL-MEFs, 105 ± 2.3. Day 3: IF-MEFs, 259 ± 7.1; CTL-MEFs, 169.5 ± 2.9. Day 4: IF-MEFs, 331 ± 8.7; CTL-MEFs, 242.5 ± 7.7. Day 5: IF-MEFs, 432.5 ± 4.7; CTL-MEFs, 301 ± 12.5. Day 6: IF-MEFs, 511.5 ± 10.02; CTL-MEFs, 374 ± 17.1. Day 7: IF-MEFs, 622.5 ± 29.3; CTL-MEFs, 430 ± 18.1. Day 8: IF-MEFs, 712.5 ± 46.6; CTL-MEFs, 486 ± 6.8.

C: Lack of response of IF-MEFs to the growth-inhibitory cytokine TGFβ. Day 1: IF-MEFs, 153 ± 5.3; CTL-MEFs, 81 ± 5.1; IF-MEFs + TGFβ, 150.5 ± 7.2; CTL-MEFs + TGFβ, 86.5 ± 4.1. Day 2: IF-MEFs, 219 ± 4.11; CTL-MEFs, 107 ± 2.7; IF-MEFs + TGFβ, 227 ± 3.8; CTL-MEFs + TGFβ, 114 ± 1.6. Day 3: IF-MEFs, 307 ± 6.9; CTL-MEFs, 153.8 ± 3.7; IF-MEFs + TGFβ, 351.5 ± 2.9; CTL-MEFs + TGFβ, 125.5 ± 4.1. Day 4: IF-MEFs, 397.4 ± 8.1; CTL-MEFs, 219 ± 7.1; IF-MEFs + TGFβ, 408.1 ± 5.5; CTL-MEFs + TGFβ, 117 ± 4.0. Day 5: IF-MEFs, 462.4 ± 4.7; CTL-MEFs, 273 ± 10.3; IF-MEFs + TGFβ, 502 ± 4.4; CTL-MEFs + TGFβ, 146.9 ± 7.4.

D: IF-MEFs are immortal. Immortalization was determined by accumulated number of population doublings over continued passages.

E: Western blotting analysis of cell cycle markers of CTL-MEFS and IF-MEFS at increasing passages.

in the S and G_2/M phases, respectively. In contrast, under the same culture conditions, the IF-MEFs displayed a higher mitotic index with a lower proportion of cells in the G_1 (46%) and S phases (7%) and a pronounced increase in the proportion of cells in G_2/M (47%) (Figure 3A). To determine if this altered cell cycle profile was indicative of altered growth, we counted the total number of IF- and CTL-MEFs during an 8 day interval and calculated the growth rate during the exponential phase of proliferation (2–4 days after plating; Figure 3B). The viability of the exponentially growing cells was approximately 95% as assessed by trypan blue dye exclusion. This analysis showed that the IF-MEFs grew significantly faster than the control fibroblasts (Figure 3B), consistent with a shortened cell cycle.

Microarray analysis revealed the downregulation in IF-MEFs of *Igf2r*, *Tsp1*, and *p57* (Figure 2B), three genes known to positively regulate transforming growth factor-β (TGFβ) activation and signaling. These gene expression changes coupled with the increased growth rates in IF-MEFs suggested a potential inability of IF-MEFs to respond to TGFβ, a pleiotropic cytokine that inhibits the growth of a diverse range of cell types (Roberts and Wakefield, 2003). To investigate whether LOI altered the ability of MEFs to respond to TGFβ growth inhibition, we exposed IF- and CTL-MEFs to TGFβ (0.1 ng/ml) 24 hr after plating. Within 48 hr, the CTL-MEFs had undergone growth arrest (Figure 3C), whereas the IF-MEFs continued to proliferate normally (Figure 3C). These results suggest that IF-MEFs were no longer responsive to the growth-inhibitory effects of TGFβ, a property shared by malignant cells.

Immortalization and transformation of IF-MEFs

Wild-type MEFs have a limited life span in cell culture and eventually undergo senescence. To determine the life span of the IF-MEFs, we used the 3T3 protocol (Todaro and Green, 1963), which involves continuous passaging of the cells. By passage 8, CTL-MEFs had undergone senescence and appeared as large, flat, nondividing cells. In contrast, IF-MEFs appeared to be spontaneously immortalized, as they maintained a constant proliferation rate and grew for at least 20 passages without showing any indication of undergoing senescence (Figure 3D). Among many of the changes associated with cellular senescence in culture is the increased expression of cell cycle regulators, such as $p16^{INK4A}$ and $p14/p19^{ARF}$, that are thought to be critical in inducing permanent G_0/G_1 arrest (Kamijo et al., 1997; Stein and Dulic, 1998). Figure 3A shows that the level of $p16^{INK4A}$ increased in later passages of IF-MEFs, comparable to that in CTL-MEFs. The $p21^{CIP1}$ cell cycle inhibitor has been shown to have a similar function as $p16^{INK4A}$ in senescing human cells, although its role in mouse cells is less clear (Brown et al., 1997; Pantoja and Serrano, 1999). Like $p16^{INK4A}$, the levels of $p21^{CIP1}$ remained constant or increased in the late passages of IF-MEFs (Figure 3E). In contrast, the level of $p19^{ARF}$ did not increase in later passages of IF-MEFs and was significantly less than in CTL-MEFs (Figure 3E). Because $p14/p19^{ARF}$ is known to bind to and sequester MDM2 and to inhibit the MDM2-dependent degradation of p53 (Sherr and Weber, 2000), we examined the level of p53 in early- and late-passage IF-MEFs. In early passages, p53 was present, but as expected from the decreased level of $p19^{ARF}$, p53 expression decreased significantly at later passages (Figure 3E).

Immortalization is an essential prerequisite for malignant transformation in mammals (Hahn and Weinberg, 2002). Therefore, we tested the transformation potential of IF-MEFs using the classic foci formation assay. This assay involves the maintenance of confluent cells over a 3 week period without passaging. In the rare incidence that a cell becomes transformed, it escapes quiescence and forms a dense outgrowth known as a focus. When CTL-MEFs were grown under these conditions,

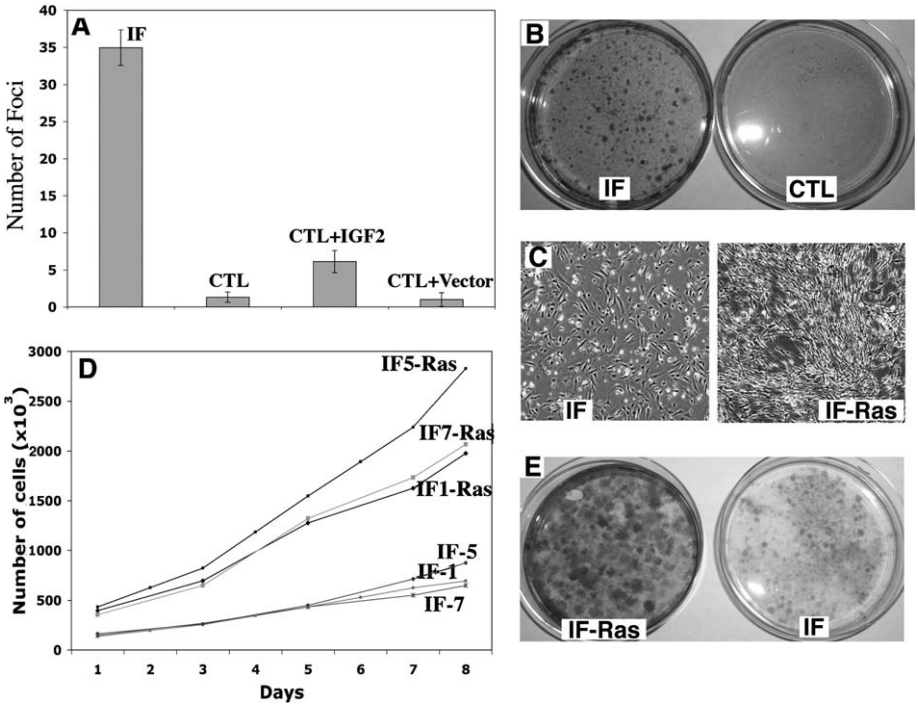

Figure 4. Transformation of IF-MEFs

A: Spontaneous transformation of IF-MEFs measured by foci assay. IF-MEFs, 34.9 ± 2.4; CTL-MEFs, 1.3 ± 0.6; CTL-*Igf2*, 6.1 ± 1.5; CTL-Vector, 1.0 ± 0.93.

B: Representative plate demonstrating the spontaneous transformation present in IF-MEF foci assay.

C: IF-MEFs infected with V12-H-Ras (IF-Ras) show altered morphology when compared to IF-MEFs (IF) alone.

D: IF-Ras-MEFs grow at a significantly faster rate than IF-MEFs.

E: Representative plate demonstrating spontaneous transformation in the low-density foci assay comparing IF, IF-LgT, and IF-Ras.

1.3 ± 0.6 foci were found per plate (Figure 4A [CTL] and Figure 4B [CTL]). In contrast, IF-MEFs formed approximately 35 ± 2.4 foci (Figure 4A [IF] and Figure 4B [IF]), consistent with LOI predisposing the IF-MEFs to spontaneous transformation.

Igf2 is an imprinted gene that often exhibits LOI and aberrant biallelic expression in human tumors (Cui et al., 2003). To determine if biallelic expression of *Igf2* was solely responsible for the immortality and the increased rate of spontaneous transformation of the IF-MEFs, we overexpressed *Igf2* in CTL-MEFs following retrovirus-mediated transduction. While *Igf2* overexpression in CTL-MEFs led to an increased growth rate, it only led to immortalization after extensive passaging as previously reported (data not shown and Hernandez et al., 2003). In the foci formation assay, *Igf2*-infected CTL-MEFs (at low passage number) formed approximately 6-fold more foci than vector-only-infected CTL-MEFs (6.1 ± 1.5 and 1 ± 0.9 foci, respectively) but failed to induce the level of spontaneous transformation observed with IF-MEFs (Figure 4A). These data combined with the Northern and microarray analysis suggest that the variable expression levels of *Igf2* contribute to the ability of the cells to spontaneously transform. However, LOI of additional genes is needed to achieve the full extent of immortalization and transformation seen in IF-MEFs.

Forced overexpression of the oncogenes SV40 Large T antigen (LgT) and a constitutively active growth signal, such as that provided by V12H-Ras, in wild-type MEFs is sufficient to cause cellular transformation. However, MEFs expressing either oncogene alone will not become transformed, but instead are either immortalized by LgT or are induced to undergo senescence by V12 H-Ras (Hahn and Weinberg, 2002). Given that the IF-MEFs displayed a greater potential for spontaneous transformation, we asked whether the effect of LOI could replace the function of either LgT or active H-Ras in this process. IF- and CTL-MEFs were infected with a LgT retroviral vector or an empty vector, and drug selection was used to select for transduced cells. The cells were plated at low density, and focus formation was assessed after a 14 day culture period. As expected, LgT-infected CTL-MEFs formed a greater number of foci as compared to the vector-only CTL-MEFs, similar to previous reports. Although the vector-only-infected IF-MEFs formed more foci than the respective CTL-MEFs, no further increase in foci numbers was observed in the LgT-infected IF-MEFs (data not shown). Thus, LOI and LgT expression do not cooperate in cellular transformation.

To ask whether LOI can replace the function of LgT and cooperate with activated H-Ras, we examined the effect of V12H-Ras expression on transformation frequency in IF-MEFs. CTL- and IF-MEFs were infected with either a V12H-Ras or an empty retrovirus vector. Expression of V12H-Ras in CTL-MEFs induced an immediate inhibition of cell growth and quiescence after passaging (data not shown), consistent with previous studies (Serrano et al., 1997). In contrast, IF-MEFs infected with V12H-Ras lost contact inhibition, exhibited a significant change in morphology, and continued to proliferate at a significantly higher rate than the vector-only control IF-MEFs (Figures 4C and 4D). In the focus formation assay, the V12H-Ras-infected IF-MEFs displayed a massive increase in focus formation compared to vector-only-infected IF-MEFs (Figure 4E). These results indicate that LOI cooperates with V12H-Ras to fully transform MEFs.

Tumor formation

The tumorigenic potential of cells was tested in vivo by subcutaneous injection into SCID mice, which lack mature lymphocytes. In this assay, fully transformed cells will form tumors beneath the skin at the site of injection. Using this assay, we

Table 1. Incidence of MEF-derived fibrosarcomas in SCID mice

MEFs	SCID mouse fibrosarcomas	
	8–12 days	4–5 months
CTL	0/6	0/6
CTL + LgT	0/6	0/6
IF	0/6	2/6
IF + LgT	0/6	2/6
IF + Ras	7/7	N/A

MEFs (2×10^6) were injected into three independent sites, and growth of tumors was assessed after the defined time point.

compared the tumorigenic potential of CTL- and IF-MEFs infected with either LgT or empty vector and IF-MEFs infected with V12H-Ras. No tumors were found in SCID mice after 4–5 months following injection with CTL-MEFs (0/7) or LgT-infected CTL-MEFs (0/7). Tumors were observed in SCID mice injected with IF-MEFs (2/6) or LgT-infected IF-MEFs (2/6) after 5 months. In contrast, all SCID mice injected with V12H-Ras-infected IF-MEFs (7/7) formed large fibrosarcomas within 14 days postinjection (Table 1). These findings are consistent with cooperation between LOI and oncogenic Ras to induce a fully transformed phenotype in MEFs. It should be noted that, due to the senescence that occurred in V12H-Ras-infected CTL-MEFs, there were insufficient cells to perform the tumor formation assay in SCID mice.

To further examine the role LOI plays in oncogenesis in vivo, we created chimeric mice using IF- and CTL-ES cell lines (using two independently derived ES cell lines for each condition). The level of chimerism contributed by the IF-ES cells ranged from 5% to 20% in the adults, whereas CTL-ES cells contributed up to 100%, as judged by coat color. Chimeras were sacrificed at 9, 12, and 18 months of age, and their tissues were examined histologically for abnormalities. Strikingly, about half of the IF chimeras at 9 months of age (n = 3/5) and all of the chimeras at 12 and 18 months of age showed the presence of hepatocellular tumors and intestinal adenomas (Table 2; Figures 5A–5E). The hepatocellular carcinomas, and in some cases adenomas, averaged approximately 5 × 6 mm in size (n = 6; data not shown) by 18 months of age. Other cancers were also observed; for instance, in one IF chimera the normal architecture of the testis was disrupted by a proliferation of homogenous cells that was consistent with testicular seminoma (Figure 5E). Another IF chimera displayed splenomegaly, and histological analysis of the bone marrow revealed a phenotype consistent with a leukemia (Figure 5D). In a 12-month-old IF chimera, a large tumor with histology consistent with lymphoma was isolated (Figure 5C). In contrast to these results, control chimeras appeared healthy at all time points and when sacrificed at 24 months of age displayed no tumors (n = 6/6; up to 100% chimerism assessed by coat color contribution).

To confirm that the cancers in the IF chimeras were derived

Table 2. The incidence of tumors in IF chimeras and after germline transmission

IF tumor incidence	9 months	12 months	18 months	24 months
Hepatocellular carcinomas	4/5	7/7	4/4	
Intestinal adenomas/carcinomas	3/5	3/3[a]	4/4	
Testicular seminoma	0/5	0/7	1/4	
Lymphoma	0/5	1/7	0/4	
Leukemia	0/5	1/7	0/4	
Tumor incidence after germline transmission				
Control			0/3	1/2
IF			0/4	0/4

[a] Three animals displayed large tumors obstructing the intestine; thorough examinations for smaller tumors in the remaining four animals were not performed.

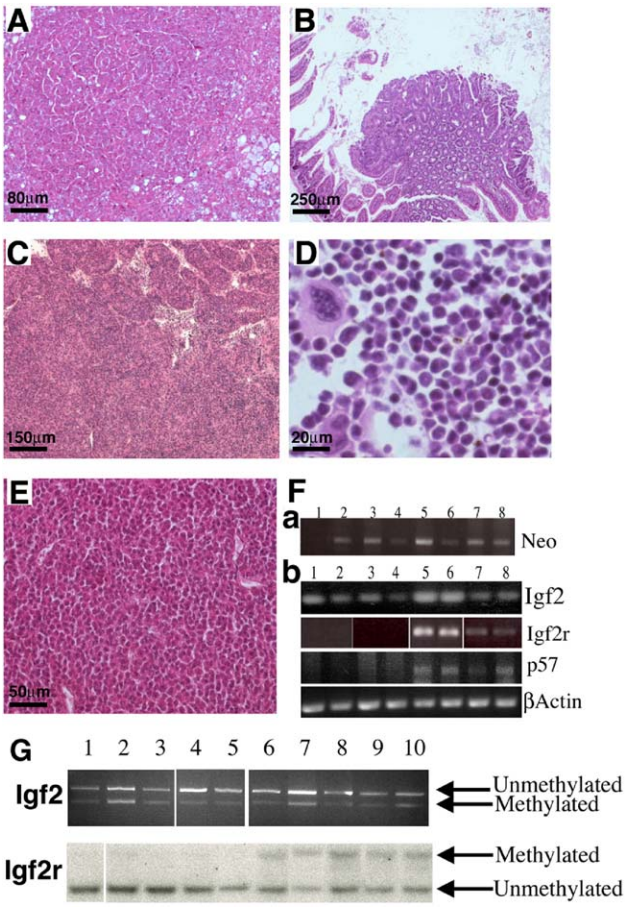

Figure 5. Histological and expression analysis of IF tumors

Histological analysis of tumor formation in IF chimeras stained with H&E. **A:** Sections of an IF hepatocellular carcinoma/adenoma. **B–E:** Intestinal adenoma/carcinoma (**B**), lymphoma (**C**), chronic myeloid-like leukemia (**D**), testicular seminoma (**E**). **Fa:** Genomic PCR to detect the presence of the IF neomycin marker gene. Lane 1, BDFI wild-type host blastocyst; lane 2, hepatocellular tumor 1; lane 3, hepatocellular tumor 2; lane 4, hepatocellular tumor 3; lane 5, testicular seminoma; lane 6, intestinal adenoma; lane 7, chronic myeloid-like leukemia; lane 8, lymphoma. **Fb:** RT-PCR expression analysis of selected imprinted genes in IF tumors. Lane 1, hepatocellular carcinoma; lane 2, testicular seminoma; lane 3, chronic myeloid-like leukemia; lane 4, lymphoma; lane 5, wild-type liver; lane 6, wild-type testis; lane 7, wild-type bone marrow; lane 8, wild-type spleen. **G:** Methylation status of selected imprinted genes in IF tumors by COBRA (Igf2) and methylation-sensitive Southern blotting (Igf2r) analysis. Lane 1, hepatocellular carcinoma; lane 2, intestinal adenoma; lane 3, testicular seminoma; lane 4, chronic myeloid-like leukemia; lane 5, lymphoma; lane 6, wild-type liver; lane 7, wild-type intestine; lane 8, wild-type testes; lane 9, wild-type spleen; lane 10, wild-type bone marrow.

from the IF-ES cells, genomic DNA from tumors was analyzed by PCR for the presence of the *neo* fragment of the β-geo gene contained in the IF-ES cells but not in the BDF1 host tissue. The *neo* gene was amplified from all of the tumors examined, consistent with an IF-ES cell origin for these neoplasms (Figure 5Fa). Taken together, tumorigenic potential of both IF-ES chimeras and IF-MEFs provides strong evidence that LOI promotes transformation both in vitro and in vivo.

In humans, the imprinted genes *p57*, *Igf2r*, and *Igf2* have been implicated in the tumorigenesis of multiple cancers (Feinberg and Tycko, 2004; Mills et al., 1998). We therefore examined the expression of these genes in tumors from the IF chimeras. Similar to our results in IF-ES cells and IF-MEFs, transcripts for *p57* and *Igf2r* were absent in the tumors (Figure 5Fb, *Igf2r*, *p57*, lanes 1–4), whereas variable levels of *Igf2* expression was found (Figure 5Fb, *Igf2*, lanes 1–4). In agreement with our findings in IF-MEFs (Figure 1D), the tumors displayed methylation of the *Igf2-H19* locus (Figure 5G, *Igf2*, lanes 1–5). These results indicate that the tumors observed in the chimeras display a loss of transcripts for the putative tumor suppressors *p57* and *Igf2r* and variable expression levels of the *Igf2* oncogene, similar to that observed in the parental IF-ES cells and IF-MEFs.

No tumors after germline transmission

Imprinted genomic methylation is established during gametogenesis (Tucker et al., 1996a), predicting that the breeding of adult IF chimeras should "reset" the methylation state and result in progeny with normal imprinting. To test whether restoration of normal imprinting would revert the tumorigenic phenotype, consistent with an epigenetic basis for these cancers, IF-chimeric mice from the two independently derived IF-ES and CTL-ES cells were crossed to C57B6 mice. Progeny inheriting the ES cell-derived genome, as determined by coat color, were aged and examined for tumors at autopsy. Careful histological analyses failed to detect tumors at 18 or 24 months of age (n = 0/8) with the exception of a single lung adenoma detected at 24 months of age (n = 1/5) in a CTL mouse (Table 2). Due to the age of this animal, this is most likely a spontaneous tumor and not caused by genetic manipulation of the parental ES cell line. The reversibility of the tumorigenic potential of IF cells following germline passage supports the epigenetic basis of these cancers and argues that tumor formation in the IF chimeras was not due to an oncogenic mutation incurred during the culturing of the ES cells.

Discussion

It has been known for some time that altered DNA methylation is associated with both benign and malignant tumor states. Considerable attention has focused on the effect of global hypo- or hypermethylation of DNA in tumors, whereas less is known about the importance of imprinting during cancer progression. The goals of this study were to engineer mice with global LOI and then examine the involvement of imprinting in tumorigenesis. By sequentially eliminating and then reestablishing *Dnmt1* expression in ES cells, we generated cells that possessed normal global DNA methylation but lacked the methylation associated with imprinting (with the exception of the *Igf2*/*H19* locus). Gene expression analyses confirmed the success of our approach, with imprinted genes being either silenced or upregulated ~2-fold in IF-MEFs compared with control cells. An analysis of the growth and cell cycle characteristics of IF-MEFs revealed that LOI conferred a number of characteristics possessed by transformed cells, including a higher growth rate, a shortened cell cycle time, cellular immortality, resistance to TGFβ, and foci formation on a confluent monolayer. Consistent with this, IF-MEFs formed tumors in SCID mice, and more significantly, adult chimeric mice derived from IF-ES cells developed tumors in multiple tissues. These data demonstrate that, in addition to regulating normal embryonic growth, imprinting plays a much wider role in tissue homeostasis by providing an essential tumor suppressor function in the adult.

Previous studies have implicated altered imprinting at the *Igf2*/*H19* locus with cancer formation. In the case of Wilms tumors in the rare Beckwith-Wiedemann syndrome, specific loss of normal imprinting on the maternal *H19* allele leads to biallelic expression of *IGF2* expression and is thought increase the number of premalignant nephrogenic precursors (Okamoto et al., 1997; Ravenel et al., 2001). In recent mouse studies, it was shown that the number of intestinal tumors that form in $Apc^{+/-}$ mutant mice was increased when *Igf2* was biallelically expressed (Sakatani et al., 2005). These studies suggested that a loss of normal imprinting at the *Igf2*/*H19* locus contributes to Wilms tumors and APC-induced intestinal tumors. However, it is unlikely that deregulated *Igf2* expression was solely responsible for the transformed phenotype observed in IF-MEFs. In our study, the *Igf2*/*H19* DMR was variably de novo methylated following reexpression of *Dnmt1*. This was an expected finding because *Igf2*/*H19* DMR, unlike other imprinted loci, has been shown to be highly susceptible to de novo methylation during cancer progression (Feinberg and Tycko, 2004), following reactivation of high levels of *Dnmt1* in $Dnmt1^{-/-}$ mutant cells (Biniszkiewicz et al., 2002), and during in vitro cultivation of preimplantation embryos (Latham et al., 1994; Mann et al., 2004). As a result of stochastic methylation at the *Igf2*/*H19* DMR in both the IF-MEFs and tumors, the expression of *Igf2* (and *H19*) was variable (ranging from normal to approximately biallelic levels in the IF-MEFs). Therefore, it is unlikely that the enhanced tumorigenic potential of cells with LOI can be solely attributed to altered expression of *Igf2*. Consistent with this, reactivating monoallelic expression of *Igf2r*, which functions in the inactivation of IGF2, only slightly reduces the level of spontaneous transformation of IF-MEFs (T.M.H. and R.J., unpublished data). Similarly, overexpression of *Igf2* in CTL-MEFs was not sufficient to induce the high rate of spontaneous transformation that was observed with IF-MEFs at low passage number (4–6), although it led to an increased growth rate. We note that, at higher passage numbers (>15), MEFs forced to overexpress *Igf2* undergo spontaneous transformation, which is likely the result of secondary mutations that accrue during extensive passaging (Hernandez et al., 2003). Based on these observations, we conclude that imprinted loci other than *Igf2*/*H19* and *Igf2r* are primarily responsible for the altered growth characteristics and transformed phenotype of cells with LOI.

Immortalization is an essential prerequisite for the formation of a tumor cell, as the introduction of an oncogene into a mammalian cell that is not immortalized will induce senescence or apoptosis due to the activation of antineoplastic defense mechanisms (Hahn and Weinberg, 2002). It is for this reason that pairs of cooperating oncogenic mutations are needed to

transform mouse cells, as the second oncogene is usually required to neutralize the protective pathways triggered by the first oncogene. For instance, overexpression of oncogenic V12H-Ras alone in MEFs leads to an upregulation of Arf and premature growth arrest. Senescence can be avoided in these cells by inhibiting the Arf-p53 pathway (Serrano et al., 1997). Similarly, our data suggest that LOI confers immortality to MEFs by inactivating the Arf-p53 pathway. Western blot analysis revealed a significant decrease in the levels of $p19^{Arf}$ and p53 in IF-MEFs. Consistent with this, overexpression of LgT in IF-MEFs, which binds to and inactivates p53, did not enhance tumor formation in the SCID assay. In contrast, overexpression of V12H-Ras in IF-MEFs failed to induce growth arrest and instead cooperated with LOI to induce tumors with short latency in SCID mice. Given the role of Arf in protecting p53 from MDM2-dependent degradation, it is possible that the reduction in p53 in IF-MEFs results indirectly from a loss of Arf. At present, the imprinted gene(s) responsible for the reduction in Arf and p53 protein levels are unknown, and further study is required for their identification.

Deregulated TGFβ signaling is a common feature of malignant cells. In the early stages of tumorigenesis, TGFβ inhibits cell growth by inducing apoptosis and arresting the cell cycle. As cells progress toward a fully malignant tumor phenotype, they become resistant to the growth-inhibiting effects of TGFβ, while other TGFβ responses remain fully operative (Roberts and Wakefield, 2003). At present, the molecular mechanisms by which cancer cells acquire this selective resistance are unclear. Our results indicate that LOI provides one mechanism by which cells can become resistant to the growth-inhibitory effects of TGFβ. At least three imprinted genes have been implicated in TGFβ signaling (Tsibris et al., 2002). TSP1 and IGF2R act as nonsignaling receptors for TGFβ and facilitate the cleavage and activation of the latent (preproprotein) ligand (Godar et al., 1999; Murphy-Ullrich and Poczatek, 2000). LOI-induced loss of *Tsp1* and *Igf2r* expression, resulting in a failure to process latent TGFβ, is unlikely to be responsible for the lack of TGFβ responsiveness, as IF-MEFs also failed to respond to active, cleaved ligand. *p57* is a more likely candidate, as this gene encodes a putative tumor suppressor that belongs to the Cip/Kip family of cyclin-dependent kinase (CDK) inhibitors and acts as a negative regulator of the cell cycle (Deshpande et al., 2005). In human hematopoietic cells, *p57* is upregulated by TGFβ and is essential for mediating its cytostatic effects on blood cells (Scandura et al., 2004). Whether p57 plays a similar role in MEFs has yet to be determined. A third possibility comes from the recent discovery that p53 plays a key role in TGFβ-induced growth arrest (Cordenonsi et al., 2003; Takebayashi-Suzuki et al., 2003). $p53^{-/-}$ MEFs show a defective cytostatic response to TGFβ and an inability to upregulate the CDK inhibitor p21WAF1 (Cordenonsi et al., 2003). Furthermore, p53 interacts with Smad2 and Smad3, downstream mediators of TGFβ signaling, where it appears to function as part of a transcriptional complex (Cordenonsi et al., 2003; Labbe et al., 2000; Liberati et al., 1999; Seoane et al., 2004). It is tempting to speculate that the mechanism by which LOI inhibits the ARF-p53 pathway to immortalize MEFs is related to its ability to confer resistance to TGFβ-induced growth arrest. Further study is required to unravel the importance of p53 in LOI-induced tumorigenesis.

Consistent with LOI rendering MEFs highly susceptible to transformation, all chimeric mice derived from IF-ES cells developed tumors in multiple tissues. This suggests that global LOI has a causal role in promoting cancer. The most common cancers were hepatocellular carcinomas and intestinal adenomas. It is unclear why this particular spectrum of cancer was observed in the IF chimera mice. It is possible, however, that tumorigenesis may be due to the dysregulation of imprinted tumor suppressor genes and oncogenes specific to each organ. The long latency of tumor development indicates that LOI sensitizes cells to cancer and that additional somatic events are required for tumor development. Offspring derived from chimeric mice that had inherited the ES cell-derived IF genome were cancer free. This indicates that the aberrant state of genomic imprinting in the IF-ES cells is fully reversible after passage through the germline, consistent with the fact that the methylation associated with imprinting can only be established in germ cells. If the tumorigenic phenotype in the LOI model was caused by a random mutational event during ES culture, then tumors would be expected to also arise in the F1 progeny. Although it is possible that an oncogene or tumor suppressor gene may have been improperly methylated (and thereby became abnormally expressed) during the generation of the IF-ES cells, we would have expected to detect such an abnormality from the microarray analysis. Furthermore, the likelihood of such an event occurring in two independently derived IF-ES cell lines but not the CTL-ES lines is small.

In summary, the ability of a cell to become immortal is a prerequisite for transformation and ultimately tumor formation. By manipulating the maintenance methylase *Dnmt1*, we were able to generate ES cells that lack the methylation marks required for maintaining imprinting, leading to global LOI. Our study provides strong evidence that LOI predisposes cells to cancer. The data support a model in which LOI at key loci encoding tumor suppressors and oncogenes provides the first step toward tumor formation by conferring cellular immortality. Furthermore, our results are consistent with subsequent genetic alterations, such as constitutive activation of a mitogenic signal, providing the next step necessary for a fully transformed phenotype both in vitro and in vivo.

Experimental procedures

2frt-flanked *Dnmt1* inactive allele

We constructed an inactive *Dnmt1* allele (2frt) by inserting a stop cassette flanked by two Frt sites between the fourth and fifth coding exons in the *Dnmt1* gene. This allele becomes reactivated following Flp-mediated recombination (Figure S1B in the Supplemental Data available with this article online).

Generation of IF and control ES cells

All experiments on live vertebrates were performed in accordance with relevant institutional and national guidelines and regulations. Massachusetts Institute of Technology's committee on animal care has approved the experiments and has confirmed that all experiments conform to the relevant regulatory standards. The most recent review and approval were received on November 4, 2004.

Mice heterozygous for the inactive 2frt *Dnmt1* allele were crossed to mice homozygous for the conditional 2loxp *Dnmt1* allele (Jackson-Grusby et al., 2001) and the ROSA26-β-geo Flp reporter allele (Possemato et al., 2002). Fertilized embryos were dissected at E0.5, cultured until the blastocyst stage, and explanted for ES cell line derivation as described (Hochedlinger and Jaenisch, 2002). ES cells were cultured as previously described (Li et al., 1992). Two independently derived ES cell lines tested positive for both the 2frt and the 2loxp *Dnmt1* alleles. These cells were exposed to Cre re-

combinase through lipofectamine-mediated, transient transfection. After short-term puromycin selection, positive clones were picked and expanded, and their genomic DNA was extracted. Clones were analyzed for Cre-mediated recombination of the *Dnmt1* (2loxp to 1loxp) allele by Southern blotting. Positive clones were expanded, and the process was repeated with exposure to Flpe recombinase to excise the stop cassette and reactivate *Dnmt1* expression. The resultant doubly recombined *Dnmt1* ES cells were termed IF (Figure 1). Control ES cells (CTL) were generated by exposure to the same recombinases but in the reverse order (Figure 1). Genomic DNA was extracted from ES cells at each stage of recombination for each *Dnmt1* genotype, 2loxp/2frt, 1loxp/2frt, 2loxp/1frt, and 1loxp/1frt. Southern blotting analysis was carried out after methylation-sensitive digestion with HpaII. Repetitive regions and elements known to be methylated were probed; these included classic centromeric satellite repeats, IAP, and LINE element (Biniszkiewicz et al., 2002) (Figure S1C).

Derivation of primary embryonic fibroblast cell lines from IF- and CTL-ES cells

MEFS were derived from day 13.5 embryos obtained by injecting IF- and CTL-ES cells into wild-type BDF1 blastocysts and implanted into foster mothers. IF- and CTL-MEFs derived from chimeric embryos were selected for two passages with the appropriate antibiotics. MEFs were frozen at passage 2 or 3 and with the exception of long-term culture were used for all experiments before passage 6. Only pure populations were used as assayed by genomic Southern blotting or PCR. MEFs and 293T ecotrophic packaging cell line were grown in DMEM supplemented with 10% FBC, 5 mM glutamine, and penicillin/streptomycin. All the cells used tested negative for mycoplasma.

Characterization of the methylation and expression status of IF- and CTL-MEFs

Genomic DNA was extracted from MEFs isolated from different chimeric fetuses, and methylation analysis of selected imprinted genes was performed by two different methods. Methylation-sensitive enzymatic digestion followed by Southern blotting was used to probe for *Igf2r* methylation (Biniszkiewicz et al., 2002). COBRA analysis was used to analyze the methylation status of *Igf2 Snrpn* and *Peg3* (Lucifero et al., 2002). Expression analysis of selected imprinted genes was carried out by two different methods using total RNA extracted from different clones of CTL- and IF-MEFs. Expression of *Igf2r*, *H19*, *Igf2*, *Peg5*, and *Grb10* was analyzed by Northern blotting using cDNA probes to the open reading frame of these genes. *P57*, *Peg1*, and *Peg3* expression was analyzed by RT-PCR using the following primers: *P57*, forward CTGACCTCAGACCCAATTCC and reverse GTTC TCCTGCGCAGTTCTCT; *Peg1* forward GCTGGGGAAGTAGCTCAGT and reverse TTTCTTCTTAGCAAGGGCCA; *Peg3* reverse CTTCTGGAAGCCGA CATTATC and forward CCTGATCAATGGGTTCCTTG; β-*actin* forward GGT CAGAAGGACTCCTATGTGG and reverse TCCCTCTCAGCTGTGGTGGT.

Microarray analysis of IF- and CTL-MEFs

Arrays were manufactured from the Mouse Genome Oligo Set V3 (Operon), which contains 31,769 oligo probes. Oligos were printed onto CodeLink Activated Slides (Amersham) using an Omnigrid 100 printer (Genemachines). Printing and postprocessing of arrays were carried out according to the manufacturer's instructions, using a modified print buffer containing 250 mM phosphate buffer (pH 8.5), with 0.00025% N-Lauroylsarcosine.

For expression profiling, 5 μg of total RNA from independent IF-MEF (n = 6) and CTL-MEF (n = 2) populations were reverse transcribed using a T7-oligo-d(T)-primer (TCTAGTCGACGGCCAGTGAATTGTAATACGACTCACTA TAGGGCGT$_{21}$N). Second strand cDNA was synthesized as previously described (Gubler and Hoffman, 1983). Double-stranded cDNAs were purified and in vitro transcribed with the Microarray RNA Target Synthesis Kit T7 (Roche). Unlabeled cRNAs were purified, and 1 μg cRNA per channel was labeled with 1 μl Cy5 or Cy3 using the Micromax ASAP RNA labeling kit (Perkin Elmer). Arrays were hybridized, washed, and dried according to the Agilent 60-mer oligo microarray processing protocol.

Arrays were scanned with a GenePix400B Scanner (Axon Instruments), and expression data were extracted by Genepix Pro 6 Software (Axon). Data normalization within and between arrays was performed with the Limma software package of the Bioconductor project (Smyth, 2004). Microarray data can be found in the Supplemental Data.

Retroviral infection assay

MEFs were infected with a high titer of retrovirus stocks produced by transient transfection of 293T cells with an ecotrophic packaging virus. pBabe-blast or pWZL-blast cells containing the retroviral infection were selected out with blasticidin. The pBabe-blast and pWZL-blast vectors containing constitutively active V12H-Ras or LgT cDNA, respectively, were both gifts of R. Weinberg (The Whitehead Institute).

Immunoblotting

Whole-cell extracts of exponentially growing cells were prepared in lysis buffer (65 mM Tris [pH 7], 1% NP40, 2 mM EDTA, 100 mM NaCl) containing the Complete cocktail of protease inhibitors (Roche), and protein concentrations were determined with the BioRad *D/C* protein assay reagent. Immunoblot analysis of p53 (Oncogene, AB-3, 1:500), p16INK4A (Santa Cruz, M-156, 1:1000), p21CIP1 (Santa Cruz, F-5, 1:1000), and p19ARF (Novus Biological, AB80-100, 1:500) was performed with 60 μg of proteins run on 12.5% acrylamide gels transferred to Immobilon-P (Millipore). Secondary antibodies coupled to HRP were purchased from Jackson ImmunoResearch Laboratories and used at 1:10,000. Detection was performed by chemiluminescence.

Growth curves, immortalization, and transformation assays

All experiments were repeated at least three times using cells from a minimum of five different fetuses for each genotype. For growth curves, 3×10^4 cells were plated into 12-well dishes and fed every second day. Serial 3T3 cultivation was conducted as described. To test the ability of the cells to form multiple layers (foci formation assay), 1×10^5 cells were plated in triplicate for each of the different genotypes and grown for 28 days; the medium was changed every second day. Plates were then fixed in ice-cold methanol and stained with cresyl violet. Low-density foci assays were conducted by plating 1.3×10^3 MEFs as described (Sage et al., 2000). To test tumorigenicity, exponentially growing cells were resuspended in PBS, and 1×10^6 cells were injected subcutaneously into SCID mice. Tumor development was monitored for up to 6 months. IF- and CTL-MEFs infected with pBabe V12H-Ras-blasticidin, pBabe-blasticidin, pWZL LgT-blasticidin, and pWZLGFP-blasticidin were selected for 3 days in 2 μg/ml blasticidin and then replated to be expanded for foci formation assays and injection into SCID mice.

TGFβ and cell cycle

Cells were plated at 3×10^4 in 12-well plates from six different embryos for each genotype in triplicate and 24 hr later were exposed to TGFβ at a concentration of 0.1 nM. Cells were then counted each day for 5 days. Cells were prepared for cell cycle analysis as described (Brugarolas et al., 1998). Samples were processed using FACScan apparatus (Becton Dickinson), and the data were analyzed using ModFit LT software (Becton Dickinson).

Generation of IF chimeric mice and histological analysis

IF and control ES cells were injected into wild-type BDF1 blastocysts. Chimeric animals were born and allowed to age for the following time points: 9, 12, and 18 months. Tumors were removed at necropsy from chimera animals and fixed in formalin for sectioning and later stained with H&E.

PCR, RT-PCR, and methylation tumor analysis

Genomic DNA from all tumors was extracted and tested for the presence of the neomycin gene using the following primers: forward AAGCCGGTCT TGTCGATCAG and reverse GATATTCGGCAAGCAGGCAT. The methylation status of genomic DNA associated with IGF2 and IGF2r was assessed by COBRA, and methylation-sensitive digestion and Southern blotting, respectively (Biniszkiewicz et al., 2002; Lucifero et al., 2002). RNA was extracted from tumors using the Qiagen RNeasy Kit, and RT-PCR was performed using the following primer pairs for these genes: Igf2 forward TGCTTCTC ATCTCTTTGGCC and reverse GGCACAGTATGTCTCCAGGA; Igf2r forward GTGTGGTATTTTTATGTATAGTTAGG and reverse AAATATCCTAAAAATAC AAACTACAC; P57 forward CTGACCTCAGACCCAATTCC and reverse GTT CTCCTGCGCAGTTCTCT; β-*actin* forward GGTCAGAAGGACTCCTATGTGG and reverse TCCCTCTCAGCTGTGGTGGT.

Supplemental data

The Supplemental Data include one supplemental figure and microarray data and can be found with this article online at http://www.cancercell.org/cgi/content/full/8/4/275/DC1/.

Acknowledgments

We thank Francis Stewart for his gift of the Flpe expression construct, Robert Weinberg for providing the LgT and V12H-Ras expression constructs, Jessie Daussman and Ruth Flannery for assistance with mice, and George Bell for computational help. This work was supported by grants from the National Institutes of Health/National Cancer Institute (5RO1 CA87869, RO1 HD 0445022, R37 CA84198 [to R.J.]).

Received: July 8, 2005
Revised: September 6, 2005
Accepted: September 26, 2005
Published: October 17, 2005

References

Baqir, S., and Smith, L.C. (2003). Growth restricted in vitro culture conditions alter the imprinted gene expression patterns of mouse embryonic stem cells. Cloning Stem Cells *5*, 199–212.

Bartolomei, M.S. (2003). Epigenetics: role of germ cell imprinting. Adv. Exp. Med. Biol. *518*, 239–245.

Baylin, S., and Bestor, T.H. (2002). Altered methylation patterns in cancer cell genomes: Cause or consequence? Cancer Cell *1*, 299–305.

Biniszkiewicz, D., Gribnau, J., Ramsahoye, B., Gaudet, F., Eggan, K., Humpherys, D., Mastrangelo, M.A., Jun, Z., Walter, J., and Jaenisch, R. (2002). Dnmt1 overexpression causes genomic hypermethylation, loss of imprinting, and embryonic lethality. Mol. Cell. Biol. *22*, 2124–2135.

Brown, J.P., Wei, W., and Sedivy, J.M. (1997). Bypass of senescence after disruption of p21CIP1/WAF1 gene in normal diploid human fibroblasts. Science *277*, 831–834.

Brugarolas, J., Bronson, R.T., and Jacks, T. (1998). p21 is a critical CDK2 regulator essential for proliferation control in Rb-deficient cells. J. Cell Biol. *141*, 503–514.

Buchholz, F., Angrand, P.O., and Stewart, A.F. (1998). Improved properties of FLP recombinase evolved by cycling mutagenesis. Nat. Biotechnol. *16*, 657–662.

Chen, R.Z., Pettersson, U., Beard, C., Jackson-Grusby, L., and Jaenisch, R. (1998). DNA hypomethylation leads to elevated mutation rates. Nature *395*, 89–93.

Cordenonsi, M., Dupont, S., Maretto, S., Insinga, A., Imbriano, C., and Piccolo, S. (2003). Links between tumor suppressors: p53 is required for TGF-β gene responses by cooperating with Smads. Cell *113*, 301–314.

Cui, H., Cruz-Correa, M., Giardiello, F.M., Hutcheon, D.F., Kafonek, D.R., Brandenburg, S., Wu, Y., He, X., Powe, N.R., and Feinberg, A.P. (2003). Loss of IGF2 imprinting: a potential marker of colorectal cancer risk. Science *299*, 1753–1755.

DeBaun, M.R., Niemitz, E.L., McNeil, D.E., Brandenburg, S.A., Lee, M.P., and Feinberg, A.P. (2002). Epigenetic alterations of H19 and LIT1 distinguish patients with Beckwith-Wiedemann syndrome with cancer and birth defects. Am. J. Hum. Genet. *70*, 604–611.

Deshpande, A., Sicinski, P., and Hinds, P.W. (2005). Cyclins and cdks in development and cancer: a perspective. Oncogene *24*, 2909–2915.

De Souza, A.T., Yamada, T., Mills, J.J., and Jirtle, R.L. (1997). Imprinted genes in liver carcinogenesis. FASEB J. *11*, 60–67.

Feinberg, A.P., and Tycko, B. (2004). The history of cancer epigenetics. Nat. Rev. Cancer *4*, 143–153.

Feinberg, A.P., and Vogelstein, B. (1983a). Hypomethylation distinguishes genes of some human cancers from their normal counterparts. Nature *301*, 89–92.

Feinberg, A.P., and Vogelstein, B. (1983b). Hypomethylation of ras oncogenes in primary human cancers. Biochem. Biophys. Res. Commun. *111*, 47–54.

Gama-Sosa, M.A., Slagel, V.A., Trewyn, R.W., Oxenhandler, R., Kuo, K.C., Gehrke, C.W., and Ehrlich, M. (1983). The 5-methylcytosine content of DNA from human tumors. Nucleic Acids Res. *11*, 6883–6894.

Gaudet, F., Hodgson, J.G., Eden, A., Jackson-Grusby, L., Dausman, J., Gray, J.W., Leonhardt, H., and Jaenisch, R. (2003). Induction of tumors in mice by genomic hypomethylation. Science *300*, 489–492.

Godar, S., Horejsi, V., Weidle, U.H., Binder, B.R., Hansmann, C., and Stockinger, H. (1999). M6P/IGFII-receptor complexes urokinase receptor and plasminogen for activation of transforming growth factor-β1. Eur. J. Immunol. *29*, 1004–1013.

Gubler, U., and Hoffman, B.J. (1983). A simple and very efficient method for generating cDNA libraries. Gene *25*, 263–269.

Hahn, W.C., and Weinberg, R.A. (2002). Modelling the molecular circuitry of cancer. Nat. Rev. Cancer *2*, 331–341.

Hernandez, L., Kozlov, S., Piras, G., and Stewart, C.L. (2003). Paternal and maternal genomes confer opposite effects on proliferation, cell-cycle length, senescence, and tumor formation. Proc. Natl. Acad. Sci. USA *100*, 13344–13349.

Hochedlinger, K., and Jaenisch, R. (2002). Monoclonal mice generated by nuclear transfer from mature B and T donor cells. Nature *415*, 1035–1038.

Jackson-Grusby, L., Beard, C., Possemato, R., Tudor, M., Fambrough, D., Csankovszki, G., Dausman, J., Lee, P., Wilson, C., Lander, E., and Jaenisch, R. (2001). Loss of genomic methylation causes p53-dependent apoptosis and epigenetic deregulation. Nat. Genet. *27*, 31–39.

Kamijo, T., Zindy, F., Roussel, M.F., Quelle, D.E., Downing, J.R., Ashmun, R.A., Grosveld, G., and Sherr, C.J. (1997). Tumor suppression at the mouse INK4a locus mediated by the alternative reading frame product p19ARF. Cell *91*, 649–659.

Kobatake, T., Yano, M., Toyooka, S., Tsukuda, K., Dote, H., Kikuchi, T., Toyota, M., Ouchida, M., Aoe, M., Date, H., et al. (2004). Aberrant methylation of p57KIP2 gene in lung and breast cancers and malignant mesotheliomas. Oncol. Rep. *12*, 1087–1092.

Labbe, E., Letamendia, A., and Attisano, L. (2000). Association of Smads with lymphoid enhancer binding factor 1/T cell-specific factor mediates cooperative signaling by the transforming growth factor-β and wnt pathways. Proc. Natl. Acad. Sci. USA *97*, 8358–8363.

Latham, K.E., Doherty, A.S., Scott, C.D., and Schultz, R.M. (1994). Igf2r and Igf2 gene expression in androgenetic, gynogenetic, and parthenogenetic preimplantation mouse embryos: absence of regulation by genomic imprinting. Genes Dev. *8*, 290–299.

Li, E., Bestor, T.H., and Jaenisch, R. (1992). Targeted mutation of the DNA methyltransferase gene results in embryonic lethality. Cell *69*, 915–926.

Li, E., Beard, C., and Jaenisch, R. (1993). Role for DNA methylation in genomic imprinting. Nature *366*, 362–365.

Liberati, N.T., Datto, M.B., Frederick, J.P., Shen, X., Wong, C., Rougier-Chapman, E.M., and Wang, X.F. (1999). Smads bind directly to the Jun family of AP-1 transcription factors. Proc. Natl. Acad. Sci. USA *96*, 4844–4849.

Lucifero, D., Mertineit, C., Clarke, H.J., Bestor, T.H., and Trasler, J.M. (2002). Methylation dynamics of imprinted genes in mouse germ cells. Genomics *79*, 530–538.

Mann, M.R., Lee, S.S., Doherty, A.S., Verona, R.I., Nolen, L.D., Schultz, R.M., and Bartolomei, M.S. (2004). Selective loss of imprinting in the placenta following preimplantation development in culture. Development *131*, 3727–3735.

Mills, J.J., Falls, J.G., De Souza, A.T., and Jirtle, R.L. (1998). Imprinted M6p/Igf2 receptor is mutated in rat liver tumors. Oncogene *16*, 2797–2802.

Murphy-Ullrich, J.E., and Poczatek, M. (2000). Activation of latent TGF-β by thrombospondin-1: mechanisms and physiology. Cytokine Growth Factor Rev. *11*, 59–69.

Ogawa, O., Eccles, M.R., Szeto, J., McNoe, L.A., Yun, K., Maw, M.A., Smith, P.J., and Reeve, A.E. (1993). Relaxation of insulin-like growth factor II gene imprinting implicated in Wilms' tumour. Nature *362*, 749–751.

Okamoto, K., Morison, I.M., Taniguchi, T., and Reeve, A.E. (1997). Epigenetic changes at the insulin-like growth factor II/H19 locus in developing kidney is an early event in Wilms tumorigenesis. Proc. Natl. Acad. Sci. USA *94*, 5367–5371.

Pantoja, C., and Serrano, M. (1999). Murine fibroblasts lacking p21 undergo senescence and are resistant to transformation by oncogenic Ras. Oncogene *18*, 4974–4982.

Possemato, R., Eggan, K., Moeller, B.J., Jaenisch, R., and Jackson-Grusby, L. (2002). Flp recombinase regulated lacZ expression at the ROSA26 locus. Genesis *32*, 184–186.

Rainier, S., Johnson, L.A., Dobry, C.J., Ping, A.J., Grundy, P.E., and Feinberg, A.P. (1993). Relaxation of imprinted genes in human cancer. Nature *362*, 747–749.

Ravenel, J.D., Broman, K.W., Perlman, E.J., Niemitz, E.L., Jayawardena, T.M., Bell, D.W., Haber, D.A., Uejima, H., and Feinberg, A.P. (2001). Loss of imprinting of insulin-like growth factor-II (IGF2) gene in distinguishing specific biologic subtypes of Wilms tumor. J. Natl. Cancer Inst. *93*, 1698–1703.

Reik, W., and Walter, J. (2001). Genomic imprinting: parental influence on the genome. Nat. Rev. Genet. *2*, 21–32.

Roberts, A.B., and Wakefield, L.M. (2003). The two faces of transforming growth factor β in carcinogenesis. Proc. Natl. Acad. Sci. USA *100*, 8621–8623.

Sage, J., Mulligan, G.J., Attardi, L.D., Miller, A., Chen, S., Williams, B., Theodorou, E., and Jacks, T. (2000). Targeted disruption of the three Rb-related genes leads to loss of G(1) control and immortalization. Genes Dev. *14*, 3037–3050.

Sakatani, T., Kaneda, A., Iacobuzio-Donahue, C.A., Carter, M.G., de Boom Witzel, S., Okano, H., Ko, M.S., Ohlsson, R., Longo, D.L., and Feinberg, A.P. (2005). Loss of imprinting of Igf2 alters intestinal maturation and tumorigenesis in mice. Science *307*, 1976–1978.

Scandura, J.M., Boccuni, P., Massague, J., and Nimer, S.D. (2004). Transforming growth factor β-induced cell cycle arrest of human hematopoietic cells requires p57KIP2 up-regulation. Proc. Natl. Acad. Sci. USA *101*, 15231–15236.

Seoane, J., Le, H.V., Shen, L., Anderson, S.A., and Massague, J. (2004). Integration of Smad and forkhead pathways in the control of neuroepithelial and glioblastoma cell proliferation. Cell *117*, 211–223.

Serrano, M., Lin, A.W., McCurrach, M.E., Beach, D., and Lowe, S.W. (1997). Oncogenic ras provokes premature cell senescence associated with accumulation of p53 and p16INK4a. Cell *88*, 593–602.

Sherr, C.J., and Weber, J.D. (2000). The ARF/p53 pathway. Curr. Opin. Genet. Dev. *10*, 94–99.

Smyth, G.K. (2004). Linear models and empirical Bayes methods for assessing differential expression in microarray experiments. Stat. Appl. Genet. Mol. Biol. *3*, 3.

Stein, G.H., and Dulic, V. (1998). Molecular mechanisms for the senescent cell cycle arrest. J. Investig. Dermatol. Symp. Proc. *3*, 14–18.

Takebayashi-Suzuki, K., Funami, J., Tokumori, D., Saito, A., Watabe, T., Miyazono, K., Kanda, A., and Suzuki, A. (2003). Interplay between the tumor suppressor p53 and TGFβ signaling shapes embryonic body axes in Xenopus. Development *130*, 3929–3939.

Todaro, G.J., and Green, H. (1963). Quantitative studies of the growth of mouse embryo cells in culture and their development into established lines. J. Cell Biol. *17*, 299–313.

Trouillard, O., Aguirre-Cruz, L., Hoang-Xuan, K., Marie, Y., Delattre, J.Y., and Sanson, M. (2004). Parental 19q loss and PEG3 expression in oligodendrogliomas. Cancer Genet. Cytogenet. *151*, 182–183.

Tsibris, J.C., Segars, J., Coppola, D., Mane, S., Wilbanks, G.D., O'Brien, W.F., and Spellacy, W.N. (2002). Insights from gene arrays on the development and growth regulation of uterine leiomyomata. Fertil. Steril. *78*, 114–121.

Tucker, K.L., Beard, C., Dausmann, J., Jackson-Grusby, L., Laird, P.W., Lei, H., Li, E., and Jaenisch, R. (1996a). Germ-line passage is required for establishment of methylation and expression patterns of imprinted but not of nonimprinted genes. Genes Dev. *10*, 1008–1020.

Tucker, K.L., Talbot, D., Lee, M.A., Leonhardt, H., and Jaenisch, R. (1996b). Complementation of methylation deficiency in embryonic stem cells by a DNA methyltransferase minigene. Proc. Natl. Acad. Sci. USA *93*, 12920–12925.

Xiong, Z., and Laird, P.W. (1997). COBRA: a sensitive and quantitative DNA methylation assay. Nucleic Acids Res. *25*, 2532–2534.